Received: 24 January 2020 | Revised: 8 December 2020 | Accepted: 9 December 2020

DOI: 10.1002/eng2.12357

RESEARCH ARTICLE

Engineering Reports Open Access WILEY

DiMIZA: A dispersion modeling based impact zone assessment of mercury (Hg) emissions from coal-fired power plants and risk evaluation for inhalation exposure

Ferhat Karaca[1,2] | **Aiganym Kumisbek**[1] | **Vassilis J. Inglezakis**[3] | **Seitkhan Azat**[4] | **Almagul Zhakiyenova**[1] | **Gulden Ormanova**[1] | **Mert Guney**[1,2]

[1]Environmental Science and Technology Group (ESTg), Department of Civil and Environmental Engineering, Nazarbayev University, Nur-Sultan, Kazakhstan

[2]The Environment & Resource Efficiency Cluster (EREC), Nazarbayev University, Nur-Sultan, Kazakhstan

[3]Chemical and Process Engineering, University of Strathclyde, Glasgow, UK

[4]Al-Farabi Kazakh National University, Almaty, Kazakhstan

Correspondence
Aiganym Kumisbek, Environmental Science and Technology Group (ESTg), Department of Civil and Environmental Engineering, Nazarbayev University, Nur-Sultan 010000, Kazakhstan.
Email: aiganym.kumisbek@nu.edu.kz

Funding information
Nazarbayev University, Grant/Award Number: 090118FD5319

Abstract

Coal-fired combined heat and power plants (CHPPs) serving large districts are among the major sources of mercury (Hg) emissions globally, including Central Asia. Most CHPPs reside on the outskirts of urban areas, thus creating risk zones. The impact of atmospheric Hg levels on health is complex to establish due to the site-specific nature of the relationship between CHPP emissions and hotspots (i.e., localized areas where Hg concentrations greatly exceed its background value). However, a methodological identification of "emission impact zones" for atmospheric Hg emissions from CHPPs with potential adverse public health outcomes has not yet been fully studied. The present work suggests an easy-to-use and cost-free impact zone identification method based on HYSPLIT dispersion modeling for atmospheric Hg emissions from CHPPs. The dispersion modeling based impact zone assessment, DiMIZA, merges short-term dispersion runs (e.g., hourly) into long-term emission impacts (e.g., yearly), which allows to identify the source impact zones. To perform a case study using the suggested method, a CHPP plant in Nur-Sultan (capital of Kazakhstan) was selected. First, traditional ad-hoc measurements were performed to identify the level of dispersions at ground level in different atmospheric stability characteristics. Then, HYSPLIT dispersion model was run for the same days and times of those particular periods when the field measurements were performed. The model results were evaluated via a comparison with the ground measurements and assessed for their atmospheric stability and diel conditions. Due to different emission loads in heating and non-heating periods, two separate pairs of impact zone maps were generated, and public Hg exposure health risks (acute and chronic) were assessed.

KEYWORDS

air pollution, atmospheric modeling, atmospheric pollution, coal combustion, human health, HYSPLIT, public health, risk characterization

1 | INTRODUCTION

Mercury (Hg) and its compounds are highly toxic to humans and the environment[1] and are classified as one of the 13 priority hazardous substances in accordance with the European Union Framework Directive.[2,3] When atmospheric Hg is inhaled, approximately 80% of it is deposited in the respiratory tract. Then, most (70%) of the deposited Hg is absorbed into the blood almost instantly, whereas the remainder is further absorbed over the course of several hours or days.[4]

During the last 100 years, there has been a 70% rise in atmospheric Hg levels due to anthropogenic emissions over natural background levels estimated prior to industrialization.[5] This increase in Hg levels represents a global threat to the health of ecosystems and humans. Due to rapid industrialization and a subsequent increase in anthropogenic activities, annual global Hg emissions rose dramatically and have reached 2000–2500 t in the 21st century. Industrial activities that contribute to the emission and release of various forms of Hg in the air include mainly coal combustion, metal extraction (e.g., gold and silver) and smelting, cement production, chlor-alkali process, and disposal of products containing Hg (e.g., lamps and batteries). In 2015, 60% of all anthropogenic Hg emissions in the atmosphere were attributed to coal combustion and artisanal gold extraction.[6-8] Geogenic Hg concentrations in coal vary widely but can be as high as 0.7–2.5 mg/kg. During coal combustion, Hg contained in coal volatilizes and enters the atmosphere in gaseous emissions. The ensuing geochemical cycle of Hg includes deposition via precipitation and conversion to highly toxic organo-Hg species prone to bioaccumulation, which might eventually impact humans through the consumption of contaminated food.

United Nations Environment Programme (UNEP) estimated Kazakhstan's total Hg emissions in 2010 as 18.7 t[9] (compared to 18.3 t in 2005[10]), 11 t of which were generated in production processes of non-ferrous metals. The second greatest contributor to national Hg emissions was coal combustion (nearly 7 t)—a major source of energy for power and heating in the country, whereas cement production and disposal of Hg-added products are responsible for most of the remaining Hg release.[9]

Existing research on Hg contamination in Kazakhstan is performed on the vicinity of industrial areas known to use Hg in their production processes (e.g., acetaldehyde and chlor-alkali plants) and does not yet include the impact from coal-fired combined heat and power plants (CHPPs) which are known major contributors to air emissions including Hg. A critical case of Hg contamination was identified in the River Nura system located in Central Kazakhstan: the source of pollution was an acetaldehyde plant, where Hg had been used as a catalyst and the resulting wastewater had been discharged without treatment. Hg level profiles in riverbed sediments and soils of riverbanks and floodplain showed localized pollution.[11,12] Hg concentrations in surface waters downstream of the source[11] as well as in the aquatic food chain raised concerns.[13] Hsiao et al.[14] confirmed that a part of the local population, which consumes fish from the river system, experienced elevated, but not severe Hg exposure levels. Another case of Hg contamination occurred in Northern Kazakhstan: a Hg-cell chlor-alkali plant in Pavlodar, which operated between 1975 and 1993 and had discharged untreated wastewater in Lake Balkyldak. Ullrich et al.[15] concluded that the lake sediments were heavily polluted and require immediate remediation. Moreover, fish from the lake were found to contain Hg concentrations above the allowable levels and was determined to be the main route for human exposure.[16] Apart from these research studies conducted on soil and water systems, to the best of our knowledge, there is no work conducted on airborne Hg concentrations and the impact of potential sources (e.g., coal-fired power plants) on the urban atmosphere in Kazakhstan.

Characterizing the levels of potentially toxic substances in the air released from point sources and subsequent identification of hotspots are important parts of inhalation risk management. Office of Environmental Health Hazard Assessment (OEHHA) suggests three Reference Exposure Level (REL) values for acute (1 hour), 8-hour, and chronic (9 years) impacts of Hg inhalation to be 0.6, 0.06, and 0.03 $\mu g/m^3$, respectively.[17] There are also international programs suggesting some guidelines and regulations for their adoption to health risk assessments.[18] The Hot Spots Analysis and Reporting Program (HARP) is one such tool to implement risk assessment.[19] Other air quality models, for example, mesoscale chemical-transport models[20] and atmospheric dispersion models[21-23] have also been used in the past to assess the general environmental quality of the area impacted by power plants. However, the available methods are time-, cost-, and resource-intensive and require a high level of computation.

Emission impact zones are the reference zones with threshold dispersion concentration levels of a specific contaminant discharged from a source. They reflect qualitatively (e.g., likelihood of being impacted) or quantitatively (e.g., potential concentrations) the possible risk zones with a scale (e.g., linear or exponential) indicating health risk for public for a selected time period. This study aims to offer a method, DiMIZA: a dispersion modeling based impact zone assessment, for identification of impact and risk zones for Hg exposure risk assessment studies on CHPP emissions based on HYSPLIT dispersion modeling. This method is used in the risk assessment study on the atmospheric gaseous (elemental)

Hg dispersion in Nur-Sultan, Kazakhstan, due to potential contribution of CHPP emissions to Hg levels. This article concludes by addressing the potential health risks due to inhalation exposure of atmospheric Hg in the city.

2 | MATERIALS AND METHODS

2.1 | Dispersion modeling and meteorological data acquisition

A dispersion modeling approach called hybrid single particle Lagrangian integrated trajectory model (HYSPLIT) was used to predict the atmospheric Hg levels over the study area. The HYSPLIT model is a complete system for computing dispersion simulations, where the dispersion of atmospheric Hg is calculated by assuming puff dispersion. This type of dispersion is a combination of the Lagrangian approach (using advection and diffusion calculations) and the Eulerian methodology (using a fixed three-dimensional grid) and is one of the most extensively used atmospheric transport and dispersion models in the field.[24] In addition to the dispersion model, relevant atmospheric meteorological data and factors, namely atmospheric Pasquill stability class characteristics, pollution distribution factors, boundary layer depth, vertical mixing coefficient, friction velocity, and horizontal mixing coefficient, were also obtained to perform the evaluation of the method's results. The meteorological data interpolated to the location of interest was obtained from the web-based Real-time Environmental Applications and Display sYstem (READY).[25]

The main parameters employed in the dispersion modeling are latitude, longitude, stack height, and a unit of Hg emission rate for plume initialization. Dispersions were calculated by assuming 1 unit (g) of Hg released into the air. The top of the model was set to average mixing height of the study area (500 m above ground level [AGL]) and the sampling level was set to 10 m AGL. Several dispersion scenarios were run by setting up the emission duration from 5 minutes to several hours and producing model output to match the Hg sampling intervals. As suggested by other researchers,[22,26] it was decided to use hourly dispersion runs as the best setup to reflect the potential impacts on the local area. Deposition (wet or dry) options were also activated in model setup.

2.2 | Identification of impact and exposure risk zones

In order to identify risk zones, the study utilized a HYSPLIT dispersion model-based method, which is free, readily available, and relatively easy-to-use. The proposed method for the identification of the qualitative risk zones is executed as follows:

1. Hourly dispersion profiles for Hg emissions were computed for the period of 1 year (n = 8760) using HYSPLIT dispersion model with the same dispersion setup described in the subsection above.
2. All gridded binary concentration files were added together (the sum function in the binary file merge option in the model) into a merged file which represents the cumulative concentration values of all runs.
3. A normalization of cumulative Hg concentration at each grid point (0.001° sensitivity) in the merged file against the maximum cumulative concentration obtained was calculated. This conversion provides the likelihood of concentration values in percentages (e.g., 100% for the maximum level, and lower values for other levels) as probabilities.
4. The merged and normalized file was later used to produce the required impact zones by scaling the percentages.

The risk zones indicating the likelihood of being impacted are presented as the contour polygons by scaling in potential impact levels (e.g., three impact likelihood levels from 1/10 to 1/1000 probabilities) of Hg emission per hour. These maps provide qualitative information and can be used to estimate potential risks by multiplying the contour values with any potential emissions. The development process of DiMIZA is summarized in Figure 1.

2.3 | Study area and source characteristics

Nur-Sultan (formerly known as Astana) is the capital of Kazakhstan located on the banks of the Ishim River in the middle of steppes and has an extreme continental climate with some of the coldest winters in the world. Heating, which is a fundamental need for survival in Nur-Sultan during long lasting winters (5 months on average), is centralized and the heating season in the city starts in October and is extended until May, if the air temperature falls below 10°C. As

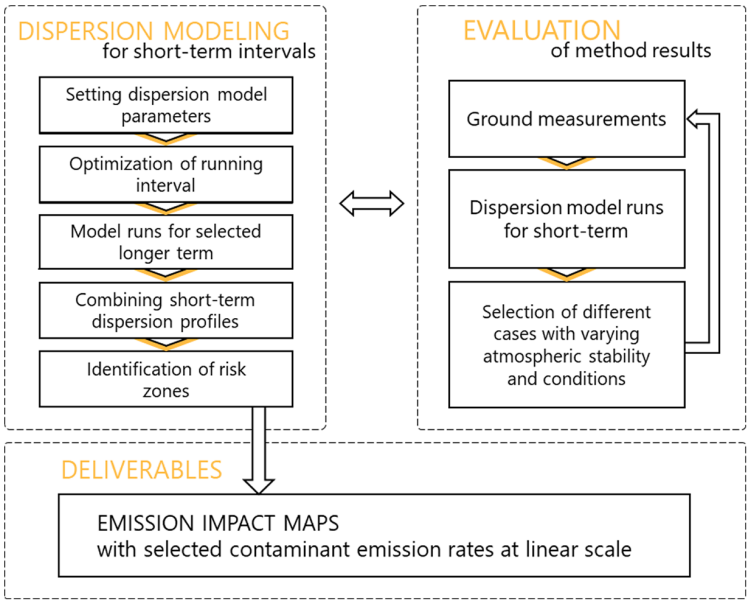

FIGURE 1 Development of the dispersion modeling based impact zone assessment (DiMIZA)

a result of coal burning and still air (air with no wind and no vertical air motion), the city experiences frequent smog episodes. Currently, CHPPs utilize the coal extracted from the open-pit mine "Bogatyr" in Ekibastuz, Kazakhstan with the reported Hg content of 16.5 μg/kg—one of the highest Hg content in coal in the country.[27] There are two state-owned CHPPs located in the urban area of Nur-Sultan City. In this study, only Akmola Coal Power Plant (CHP-2, located at the coordinates: 51.1893N, 71.5097E) with an electric power production capacity of 340 MWe was used as a case study application. The emission control technologies at CHP-2 are limited to wet fly ash collectors and a hydraulic ash removal system, which may be ineffective in reducing gaseous Hg emissions from coal combustion. The coal consumption of the city by the CHPPs is estimated to be 3.7 million tons per year.[28]

2.4 | Hg measurements

Ground level measurements conducted to evaluate the dispersion model results were performed during three campaigns in June and July of 2019 in the non-heating period to eliminate other emissions related to district heating. These measurements were performed using a traditional ad hoc sampling strategy to identify the levels of dispersion in different atmospheric stability characteristics.[29] The ground measurement campaigns started at the center of Hg emission dispersion location, extended to the outer distances up to a few kilometers in upwind directions, and ended when the urban background levels were observed (effective dispersion distance). The atmospheric Hg concentrations were measured using a portable Hg Analyzer (Lumex RA-915M) which works based on the absorption of the 254-nm resonance radiation by Hg atoms using Zeeman correction for background absorption (atomic absorption spectrometry coupled with a high frequency modulation of light polarization [ZAAS-HFM]) with a detection limit of 0.5 ng/m^3. Since the analyzer must always operate in a temperature-controlled environment, the device was installed in a vehicle with an air-conditioning system set at 17°C during the campaigns and connected to a tube with an outlet attached to the window opening. Each measurement was done by stopping at the sampling locations for several minutes to obtain a stable reading, as the device was preset to collect Hg concentration data with an interval of 1 second, and the average values of a measurement duration of 3 minutes have been reported. The instrument was calibrated before and after the campaigns as well as every 10 minutes using an internal calibration cell and was operating in the continuous measurement mode.

3 | RESULTS AND DISCUSSION

3.1 | Field campaigns

Three field measurement campaigns were carried out under different atmospheric stability and meteorological conditions during the non-heating period in Nur-Sultan City. These measurements were conducted to evaluate the agreement level

of the dispersion model results with the ground level concentrations. Measurement results of the sampling as well as meteorological conditions are summarized in Table 1. The overall average for ambient total gaseous Hg concentration was 6.0 ± 1.8 ng/m^3, and different urban averages were observed in different campaigns ranging from 5.6 to 7.3 ng/m^3. Measured levels were consistently higher in locations closer (around 2 km) to the CHPP supporting the suggestion that the plant is the main source of atmospheric Hg, whereas the urban background measurements stayed at similar levels during all campaigns in Nur-Sultan City.

Urban background sampling point is always the same location, 10 km away from the source in minimally impacted city outskirts. The measured urban background Hg level was 4 ng/m^3. This value is higher than or equal to those of most of the European cities (0.1–5 ng/m^3), at the same level with those of some South and East Asian urban measurements (e.g., Seoul [3.22–5.26 ng/m^3]), and lower than several cities in China (e.g., Guiyang [7.40–9.72 ng/m^3], Beijing [7.9–34.9 ng/m^3], Changchun [18.4 ng/m^3]).[30-32] Kumari et al.[30] attributed much higher Hg levels in Indian cities (e.g., Bhilai, 140–1830 ng/m^3) than the others (e.g., those in China, Korea, and Japan) to the reason that most of the studies on Hg concentrations in Indian cities were carried out in the vicinity of coal-fired power plants. The present study also finds higher Hg levels at the locations closer to the CHPP, but still not as elevated as in some of the cities mentioned.

Atmospheric stability analyses were performed to identify the relative importance of the point source on the observed Hg concentrations. Table 1 reports the atmospheric stability data for the specific times of the measurement campaigns, and Figure S1 (supplementary material) illustrates the diel analysis of the campaign periods. All the values are presented for UTC time (Nur-Sultan's local time is UTC + 6). The field campaigns represent significantly different meteorological and dispersion conditions. The first campaign was carried out when atmospheric stability was at level "C" with slower vertical and horizontal mixing coefficients, which are less favorable conditions for dispersion compared to the second campaign (level "A"). However, diel atmospheric stability data analysis showed that such conditions in the city do not last more than half a day as demonstrated by the vertical mixing coefficients (Figure S1). Significant changes in wind direction and stability throughout daily cycles are typical in Nur-Sultan leading to a higher level of pollution for several

TABLE 1 Summary of prevailing meteorological characteristics during field campaigns

Parameter and characteristics	Campaign 1	Campaign 2	Campaign 3
Date and time (UTC)	June 21, 2019 06Z (Daytime)	July 1, 2019 06Z (Daytime)	July 16, 2019 15 UTC (Nighttime)
Average Hg concentration and Urban background level (ng.m^{-3})	7.3 4	5.7 4	5.6 4
Weather conditions: Temperature Conditions Humidity Pressure Wind Direction Wind speed	19 °C Partly sunny 74% 1010 mbar NNE 19 km/h	24 °C Sunny 53% 1015 mbar ESE 27 km/h	32 °C Sunny 47% 1008 mbar E 12 km/h
Pasquill Stability Class[a]	C	A	D
Boundary layer depth, meters above model terrain (Zi)	1507	1191	116 (lower than the stack height)
Vertical (Kz) and horizontal (Kh) mixing coefficients (m^2 s^{-2})	52.2 10,330	162.2 15,410	21.4 6130
Stack plume type	Coning	Looping	Fanning
Observations	Windy on the ground, the stack plume was considerably visual, thick, and dispersing with a cone shape over the city in the western direction.	High wind speed on the ground, stack plume was slightly visual and dispersing over the northern outskirts of the city (the NW direction of the plant)	Just before the field monitoring, the stack plume was visible on Southwest (SW) direction over the left bank. After sunset, the plume shape dispersed over the city making a straight layer of smoke over a few hundred meters on the East direction

[a] A: Extremely unstable conditions, B: Moderately unstable conditions, C: Slightly unstable conditions, D: Neutral conditions, E: Slightly stable conditions, F: Moderately stable conditions, G: Extremely Stable.

hours to the urban space due to diurnal variability in wind direction. Nighttime periods are always more stable with very low atmospheric boundary layer heights, which are routinely lower than 500 m in summer periods. Due to lower mixing heights, Hg concentrations are expected to be the highest at night and in the early morning; however, it was not the case in the nighttime campaign (Campaign 3). The main reason of having moderately elevated, but not extreme ground level concentrations during the nighttime measurements was attributed to the efficient stack height effect of the power plant. The field observations support that a lofting plume (also known as a fanning plume) occurred above the surface inversion layer which was estimated to be less than 150 m efficient stack height (Table 1).

The variations of the atmospheric stability characteristics of the campaigns revealed that the ground level Hg observations are significantly related not only to the point source emissions but also to the meteorological changes in atmospheric stability and mixing height. Higher concentrations were observed during stable conditions with a coning plume (Campaign 1) and the level of impact with looping plume gets less significant with the unstable conditions (Campaign 2). The Hg concentrations have been fairly different between different campaigns whereas background locations during different campaigns had similar concentrations. The maximum urban concentrations typically occur during stable atmospheric conditions before lofting plume occurs during the sunset times and then the city atmosphere experiences lower concentrations reaching minimum levels in the afternoon. These diurnal dynamics have been attributed to nighttime inversion with stable nocturnal atmospheric conditions followed by daytime inversion breakups when the sun warms the ground.

3.2 | Evaluation of results by ground level measurements and observations

Atmospheric Hg dispersion concentrations were computed using HYSPLIT dispersion model for the time periods of the field campaigns. The dispersion results were visualized in Figure 2 where the colored areas represent 1 (yellow), 1/10

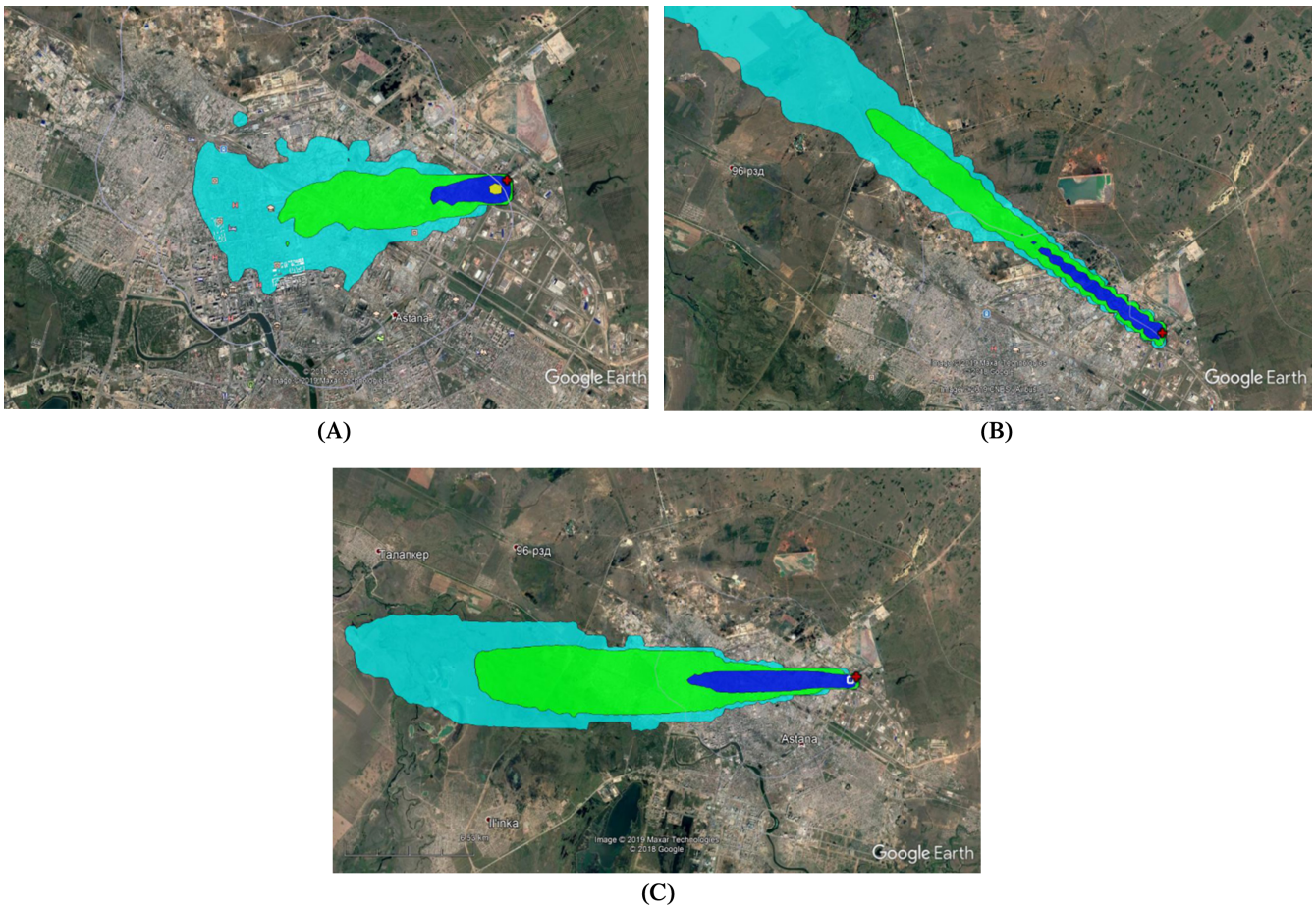

FIGURE 2 Dispersion model results for Case 1 (June 21, 2019: UTC time 5:00–9:00), Case 2 (July 1, 2019: UTC time 5:00–9:00), and Case 3 (July 16, 2019 UTC time 15:00–19:00). Emission rate: 5.81 g Hg/hr. Concentrations from inner to outer contours: 5.0, 0.5, 0.05, 0.005 ng/m^3

(blue), 1/100 (green), and 1/1000 (light blue) nano units per cubic meter concentrations from inner to outer counters. Outputs of the model simulations were presented as an overlay in Google Earth to compare the modeled plume with the field observations (Table 1) and field measurements. The results of the dispersion modeling and ground level measurements have a good agreement, and the effect of the stack plume over the ground level is also clearly observed in the field and was in agreement with the model on the upwind direction of the power plant. During the field campaigns, Hg concentrations in the blue zone reached 9 and 11 ng/m^3, which were 5 to 7 ng/m^3 higher than the urban background levels (outside of the light blue zone). Overall, the ground-level atmospheric measurements reasonably match with the dispersion model results.

3.3 | Identification of the impact and exposure risk zones

A single dispersion model and/or interpolation maps of ground level pollution levels cannot provide an accurate estimate of the potential impact zones of any point source, if the risk assessment aims for a longer time period (e.g., yearly or seasonal). In addition, to perform a more accurate risk assessment for long-term impacts, the identification of risk (or impact) zones is important. Risk zones are reference zones with a specific concentration level of the contaminant of interest, at which the potential exposure level can become unhealthy for public. DiMIZA deals with this task by combining hourly dispersion model results into one merged file for any selected longer time period (e.g., heating, non-heating, or yearly).

This method suggests generating emission impact zones of a potential source (e.g., a power plant) as scaled contour polygons (e.g., from 1/10 to 1/1000 probabilities of being impacted by Hg emission) for the selected long-term periods (e.g., heating or non-heating). These levels can be reasonably used to assess the potential impact of the selected source for public health risk assessment, which is further discussed in the following subsection. A comparable but more complex recent method called HyADS[33] also exists that combines HYSPLIT trajectory dispersion model runs. HyADS has a different aim compared to DiMIZA, which is to study greater areas and a number of potential sources for increased study durations. The method includes simplified fate and transport estimations and a focus on impact zones (but not on resultant concentrations) with a quantitative outcome. Our presented model DiMIZA focuses on the local effect (i.e., short-term dispersion for emissions from a singular source) with a semi-quantitative (%) outcome.

In Nur-Sultan City, central heating systems are regulated to be operational, if the average daily outdoor air temperature remains at 10°C and lower for 5 days. The middle of May was selected as the start of the non-heating period and it was assumed that the non-heating period ended at the beginning of October. Thus, 46% and 54% of the data were separated as non-heating and heating periods sub-datasets, respectively. Based on the coal consumption data provided in Section 2.3 and further assuming that (i) the annual total emission from heating season is twice as much as the non-heating period and that (ii) the coal contains 13.7 μg/kg (a conservative estimate that corresponds to 75th percentile value of coal Hg concentrations from different coal mines in Kazakhstan according to Ilyushchenko and Uskov[27]), the hourly Hg emissions during non-heating and heating periods were calculated as 4.2 g and 7.2 g Hg per hour, correspondingly. Figure 3 displays separate impact risk zone maps for heating and non-heating periods, since the district heating requires great amount of heat energy increasing subsequent atmospheric Hg emissions significantly during heating season.

(A) (B)

FIGURE 3 Likelihood of impacts per total Hg emission for heating and non-heating periods in Nur-Sultan (Astana)

The impact and risk zones in the heating season are larger than the non-heating period, however, the non-heating impact zones, especially the highest impact counter (1/10 impact zone), are more dispersed over the urban structure in South-West direction.

3.4 | Inhalation risk assessment and potential implementations

The reference concentration (RfC) value for possible risks due to inhalation exposures of atmospheric Hg based on the lowest-observed-adverse-effect-level (LOAEL) is 0.3 μg/m^3.[34] This RfC value is significantly higher than the measured concentrations in Nur-Sultan City, so it can be regarded as unlikely to lead to direct adverse health effects. The RfC value of 0.3 μg/m^3 was obtained from human occupational studies in the workplace and does not indicate a reference value for deleterious non-cancer effects for long-term exposures during a lifetime.

The obtained results also suggest that atmospheric Hg levels out of the exposure risk zones (about 3 km away from the point source) do not depend only on the emission strength but also significantly on atmospheric stability conditions, especially wind speed and inversion layer height. As a result, it might be unlikely to experience elevated atmospheric Hg levels at the ground level in some of the densely populated locations (e.g. Northwestern part of the city which falls largely into the 1/100th and 1/1000th impact zones).

When the power plant is operated at its maximum capacity during longer time periods under stagnant (or not changing) dispersion characteristics (e.g., several days during the winter period), more extreme values can be experienced for a shorter period. This hypothesis can be tested by performing field measurements during anticyclone stagnation periods in winter.

4 | CONCLUSION

The present study offers a new method, DiMIZA: a Dispersion modeling based impact zone assessment, for the identification of the emission impact zones and health risk zones for mercury (Hg) exposure risk assessment studies for CHPP emissions based on HYSPLIT dispersion modeling. A case assessment was also performed for Nur-Sultan City (Kazakhstan). The dispersion variations of gaseous Hg under different meteorological and atmospheric stability conditions were evaluated by discussing the source dependent (e.g., the plant's location, emission characteristics, and fuel quality) and independent (e.g., atmospheric Pasquill stability class characteristics, pollution distribution factors, and boundary layer depth) factors. The field measurements were conducted during non-heating period to eliminate other district heating-related emissions, so the contribution of Hg to the urban atmosphere could only be attributed to CHPP emissions in the study area. The main advantages of the proposed method among existing models are that it is free, readily available, and relatively simple. In general, the results here presented indicate the potential of HYSPLIT based dispersion modeling as a tool for an improved understanding of the impacts of power plants and their impact and risk zones. The risk assessment performed in the present study is only a preliminary atmospheric Hg exposure risk assessment of Nur-Sultan since it does not include numerous other coal emissions (e.g., other CHPP operating during the heating season, private boilers, and district heating emissions). Thus, one can expect to have significantly higher or different levels of urban Hg concentrations during heating periods in various locations. The scope of this research is limited to only one potential source (a CHPP). In order to assess the temporal and spatial atmospheric Hg variations with a complete inhalation risk assessment, further research is required by including all possible emission sources in all periods.

ACKNOWLEDGMENTS

The authors acknowledge the financial support provided by Nazarbayev University's Faculty Development Competitive Research Grant Program (FDCRGP, funder project reference: 090118FD5319). The authors also gratefully acknowledge NOAA Air Resources Laboratory (ARL) for the provision of HYSPLIT transport and dispersion model and/or READY website (http://www.ready.noaa.gov) used in this publication.

PEER REVIEW INFORMATION

Engineering Reports thanks the anonymous reviewers for their contribution to the peer review of this work.

DATA AVAILABILITY STATEMENT

The data that support the findings of this study are available from the corresponding author upon reasonable request.

CONFLICT OF INTEREST

The authors declare that they have no conflict of interest.

ORCID

Aiganym Kumisbek https://orcid.org/0000-0003-4986-0522

REFERENCES

1. European Environment Agency (EEA). *Hazardous Substances in Europe's Fresh and Marine Waters*. Luxembourg: Publications Office of the European Union; 2011 https://doi.org/10.2800/78305.
2. European Commission (EC). Directive 2000/60/EC of the European Parliament and the council. *Off J Eur Communities*. 2000;22:L327 http://data.europa.eu/eli/dir/2000/60/oj.
3. European Commission (EC). Directive 2008/105/EC of the European Parliament and the council. *Off J Eur Communities*. 2008;24:L348 http://data.europa.eu/eli/dir/2008/105/oj.
4. Leggett RW, Munro NB, Eckerman KF. Proposed revision of the ICRP model for inhaled mercury vapor. *Health Phys*. 2001;81:450-455. https://doi.org/10.1097/00004032-200110000-00010.
5. Gaffney J, Marley N. In-depth review of atmospheric mercury: sources, transformations, and potential sinks. *Energy Emiss Control Technol*. 2014;2:1-21. https://doi.org/10.2147/EECT.S37038.
6. Mazyck DW, Hagan AM, Byrne H. Aqueous phase mercury removal: strategies for a secure future water supply. Critical national need idea white paper. National Institute for Standards and Instrumentation, US Department of Commerce. 2009. http://www.nist.gov/tip/wp/pswp/upload/137_aqueous_phase_mercury_removal_strategies.pdf.
7. United Nations Environment Programme (UNEP). *Global Mercury Assessment 2018*. Geneva: Chemicals and Health Branch; 2019 https://www.unenvironment.org/resources/publication/global-mercury-assessment-2018.
8. United States Environmental Protection Agency (USEPA). *Treatment Technologies for Mercury in Soil, Waste, and Water*. Washington: U.S. EPA Office of Superfund Remediation and Technology Innovation; 2007 https://www.epa.gov/remedytech/treatment-technologies-mercury-soil-waste-and-water.
9. Arctic Monitoring and Assessment Programme (AMAP)/United Nations Environment Programme (UNEP). Technical Background Report for the Global Mercury Assessment 2013. 2013.
10. Arctic Monitoring and Assessment Programme (AMAP)/United Nations Environment Programme (UNEP). Technical Background Report to the Global Atmospheric Mercury Assessment. 2008.
11. Heaven S, Ilyushchenko MA, Tanton TW, Ullric SM, Yanin EP. Mercury in the River Nura and its floodplain, Central Kazakhstan: I River sediments and water. *Sci Total Environ*. 2000a;260:35-44. https://doi.org/10.1016/S0048-9697(00)00540-4.
12. Heaven S, Ilyushchenko MA, Kamberov IM, et al. Mercury in the River Nura and its floodplain, Central Kazakhstan: II. Floodplain soils and riverbank silt deposits. *Sci Total Environ*. 2000b;260:45-55. https://doi.org/10.1016/S0048-9697(00)00566-0.
13. Ullrich SM, Ilyushchenko MA, Uskov GA, Tanton TW. Mercury distribution and transport in a contaminated river system in Kazakhstan and associated impacts on aquatic biota. *Appl Geochem*. 2007a;22:2706-2734. https://doi.org/10.1016/j.apgeochem.2007.07.005.
14. Hsiao HW, Ullrich SM, Tanton TW. Burdens of mercury in residents of Temirtau, Kazakhstan. I: Hair mercury concentrations and factors of elevated hair mercury levels. *Sci Total Environ*. 2010;409:2272-2280. https://doi.org/10.1016/j.scitotenv.2009.12.040.
15. Ullrich SM, Ilyushchenko MA, Kamberov IM, Tanton TW. Mercury contamination in the vicinity of a derelict chlor-alkali plant. Part I: sediment and water contamination of Lake Balkyldak and the river Irtysh. *Sci Total Environ*. 2007b;381:1-16. https://doi.org/10.1016/j.scitotenv.2007.02.033.
16. Ullrich SM, Ilyushchenko MA, Tanton TW, Uskov GA. Mercury contamination in the vicinity of a derelict chlor-alkali plant. Part II: contamination of the aquatic and terrestrial food chain and potential risks to the local population. *Sci Total Environ*. 2007c;381:290-306. https://doi.org/10.1016/j.scitotenv.2007.02.020.
17. Office of Environmental Health Hazard Assessment (OEHHA). Technical Support Document for the Derivation of Noncancer Reference Exposure Levels. 2008. https://oehha.ca.gov/media/downloads/crnr/noncancertsdfinal.pdf. Accessed October 29, 2020.
18. Office of Environmental Health Hazard Assessment (OEHHA). Notice of Adoption of Air Toxics Hot Spots Program Guidance Manual for the Preparation of Health Risk Assessments 2015. 2015. https://oehha.ca.gov/air/crnr/notice-adoption-air-toxics-hot-spots-program-guidance-manual-preparation-health-risk-0. Accessed July 17, 2019.
19. Office of Environmental Health Hazard Assessment (OEHHA). Acute, 8-hour and Chronic Reference Exposure Level (REL) Summary. 2016. https://oehha.ca.gov/air/general-info/oehha-acute-8-hour-and-chronic-reference-exposure-level-rel-summary. Accessed July 3, 2019.
20. Piersanti A, Adani M, Briganti G, et al. Air quality modeling and inhalation health risk assessment for a new generation coal-fired power plant in Central Italy. *Sci Total Environ*. 2018;644:884-898. https://doi.org/10.1016/j.scitotenv.2018.06.393.
21. Dinis ML, Fiuza A, Gois J, et al. Modeling radionuclides dispersion and deposition downwind of a coal-fired power plant. *Procedia Earth Planet Sci*. 2014;8:59-63. https://doi.org/10.1016/j.proeps.2014.05.013.

22. Mokhtar MM, Hassim MH, Taib RM. Health risk assessment of emissions from a coal-fired power plant using AERMOD modelling. *Process Saf Environ Prot*. 2014;92:476-485. https://doi.org/10.1016/j.psep.2014.05.008.
23. Salloum S, Nassar J, Baalbaki R, Shihadeh AL, Saliba NA, Lakkis I. PM10 Plume dispersion data of the Zouk power plant in Lebanon. *Data Brief*. 2018;20:1905-1911. https://doi.org/10.1016/j.dib.2018.09.047.
24. Ngan F, Stein A, Finn D, Eckman R. Dispersion simulations using HYSPLIT for the Sagebrush Tracer Experiment. *Atmos Environ*. 2018;186:18-31. https://doi.org/10.1016/j.atmosenv.2018.05.012.
25. Rolph G, Stein A, Stunder B. Real-time environmental applications and display sYstem: READY. *Environ Model Softw*. 2017;95:210-228. https://doi.org/10.1016/j.envsoft.2017.06.025.
26. Milando CW, Martenies SE, Batterman SA. Assessing concentrations and health impacts of air quality management strategies: framework for rapid emissions scenario and health impact ESTimation (FRESH-EST). *Environ Int*. 2016;94:473-481. https://doi.org/10.1016/j.envint.2016.06.005.
27. Ilyushchenko MA, Uskov GA. Environmental mercury pollution: mercury emissions, remediation and health effects. Astana: Proceedings of International Workshop. 2007. http://hg-kazakhstan.narod.ru/pdf/BookE.pdf. Accessed August 11, 2019.
28. Serikov D. Потребление богатырского угля на ТЭЦ Астаны выросло на 16%. 2018. https://inbusiness.kz/ru/last/potreblenie-bogatyrskogo-uglya-na-tec-astany-vyroslo-na-16. Accessed November 21, 2019.
29. Metallo MC, Poli AA, Diana M, Persia F, Cirillo MC. Air pollution loads on historical monuments: an air quality model application to the marble Arch of Titus in Rome. *Sci Total Environ*. 1995;171:163-172. https://doi.org/10.1016/0048-9697(95)04690-0.
30. Kumari A, Kumar B, Manzoor S, Kulshrestha U. Status of atmospheric mercury research in South Asia: a review. *Aerosol Air Qual Res*. 2015;15:1092-1109. https://doi.org/10.4209/aaqr.2014.05.0098.
31. Loahmann E, Munari S, Amicarelli V, Abbaticchio P. *Heavy Metals: Identification of Air Quality and Environmental Problems in the European Community*. Vol 1 and 2 (Reports No. EUR 10678 EN/I and EUR l0678 EN/II). Luxembourg: Commission of the European Communities; 1986.
32. Wangberg I, Munthe J, Pirrone N, et al. Atmospheric mercury distribution in Northern Europe and in the Mediterranean region. *Atmos Environ*. 2001;35:3019-3025. https://doi.org/10.1016/S1352-2310(01)00105-4.
33. Henneman LRF, Choirat C, Ivey C, Cummiskey K, Zigler CM. Characterizing population exposure to coal emissions sources in the United States using the HyADS model. *Atmos Environ*. 2019;203:271-280. https://doi.org/10.1016/j.atmosenv.2019.01.043.
34. United States Environmental Protection Agency (USEPA). *Integrated Risk Information System (IRIS) for Mercury, Elemental (CASRN 7439-97-6)*. Washington, DC: National Center for Environmental Assessment, Office of Research and Development; 1995 www.epa.gov/iris/subst/0370.htm.

SUPPORTING INFORMATION

Additional supporting information may be found online in the Supporting Information section at the end of this article.

How to cite this article: Karaca F, Kumisbek A, Inglezakis VJ, et al. DiMIZA: A dispersion modeling based impact zone assessment of mercury (Hg) emissions from coal-fired power plants and risk evaluation for inhalation exposure. *Engineering Reports*. 2021;3:e12357. https://doi.org/10.1002/eng2.12357